Atmos. Chem. Phys., 11, 3713–3730, 2011
www.atmos-chem-phys.net/11/3713/2011/
doi:10.5194/acp-11-3713-2011

Atmospheric Chemistry and Physics

Exploring causes of interannual variability in the seasonal cycles of tropospheric nitrous oxide

C. D. Nevison[1], E. Dlugokencky[2], G. Dutton[2,3], J. W. Elkins[2], P. Fraser[4], B. Hall[2], P. B. Krummel[4], R. L. Langenfelds[4], S. O'Doherty[5], R. G. Prinn[6], L. P. Steele[4], and R. F. Weiss[7]

[1]University of Colorado, Institute for Arctic and Alpine Research, Boulder, Colorado, USA
[2]NOAA Earth System Research Laboratory, Global Monitoring Division, Boulder, Colorado, USA
[3]University of Colorado, Cooperative Institute for Research in Environmental Sciences, Boulder, Colorado, USA
[4]Centre for Australian Weather and Climate Research/CSIRO Marine and Atmospheric Research, Aspendale, Victoria, 3195, Australia
[5]School of Chemistry, University of Bristol, Bristol, UK
[6]Center for Global Change Science, Department of Earth, Atmospheric, and Planetary Science, Massachusetts Institute of Technology, Cambridge, MA 02139-4307, USA
[7]Scripps Institution of Oceanography, University of California, San Diego, La Jolla, CA , USA

Received: 17 September 2010 – Published in Atmos. Chem. Phys. Discuss.: 3 November 2010
Revised: 4 March 2011 – Accepted: 7 April 2011 – Published: 21 April 2011

Abstract. Seasonal cycles in the mixing ratios of tropospheric nitrous oxide (N_2O) are derived by detrending long-term measurements made at sites across four global surface monitoring networks. The detrended monthly data display large interannual variability, which at some sites challenges the concept of a "mean" seasonal cycle. In the Northern Hemisphere, correlations between polar winter lower stratospheric temperature and detrended N_2O data, around the month of the seasonal minimum, provide empirical evidence for a stratospheric influence, which varies in strength from year to year and can explain much of the interannual variability in the surface seasonal cycle. Even at sites where a strong, competing, regional N_2O source exists, such as from coastal upwelling at Trinidad Head, California, the stratospheric influence must be understood to interpret the biogeochemical signal in monthly mean data. In the Southern Hemisphere, detrended surface N_2O monthly means are correlated with polar spring lower stratospheric temperature in months preceding the N_2O minimum, providing empirical evidence for a coherent stratospheric influence in that hemisphere as well, in contrast to some recent atmospheric chemical transport model (ACTM) results. Correlations between the phasing of the surface N_2O seasonal cycle in both hemispheres and both polar lower stratospheric temperature and polar vortex break-up date provide additional support for a stratospheric influence. The correlations discussed above are generally more evident in high-frequency in situ data than in data from weekly flask samples. Furthermore, the interannual variability in the N_2O seasonal cycle is not always correlated among in situ and flask networks that share common sites, nor do the mean seasonal amplitudes always agree. The importance of abiotic influences such as the stratospheric influx and tropospheric transport on N_2O seasonal cycles suggests that, at sites remote from local sources, surface N_2O mixing ratio data by themselves are unlikely to provide information about seasonality in surface sources, e.g., for atmospheric inversions, unless the ACTMs employed in the inversions accurately account for these influences. An additional abioitc influence is the seasonal ingassing and outgassing of cooling and warming surface waters, which creates a thermal signal in tropospheric N_2O that is of particular importance in the extratropical Southern Hemisphere, where it competes with the biological ocean source signal.

Correspondence to: C. D. Nevison
(nevison@colorado.edu)

Published by Copernicus Publications on behalf of the European Geosciences Union.

1 Introduction

Nitrous oxide (N_2O) is an important greenhouse gase with a global warming potential about 300 times that of CO_2 (Forster et al., 2007). It is the major source of NO to the stratosphere and, with the decline of chlorofluorocarbons (CFCs) in the atmosphere, is the dominant ozone-depleting substance emitted in the 21st century (Ravishankara et al., 2009). The atmospheric N_2O concentration has risen from about ∼270 ppb preindustrially to ∼320 ppb today (MacFarling-Meure et al., 2006), where the units of ppb (parts per billion) are used as a convenient shorthand for mole fractions in nanomoles of N_2O per mole of dry air. Some of the best information about the global budget of atmospheric N_2O has been derived from direct atmospheric monitoring, which has allowed the detection of long-term concentration trends and hence the inference of the relative strength of natural versus anthropogenic sources (Weiss, 1981; Prinn et al., 2000; Hirsch et al., 2006). Natural microbial production is known to account for about 2/3 of N_2O emissions, but partitioning of this production between soils and oceans is uncertain. Anthropogenic sources are primarily associated with agriculture, either directly (e.g., emissions from fertilized fields) or indirectly (e.g., emissions from estuaries polluted with fertilizer runoff) (Forster et al., 2007). It is unclear to what extent anthropogenic emissions can be mitigated in the future, given the need to feed the expanding human population (Kroeze et al., 1999; Mosier et al., 2000).

While large uncertainties remain in bottom-up efforts to quantify N_2O sources, the precision of direct atmospheric N_2O measurements has improved to the point where small-amplitude seasonal cycles (currently in the range of 0.1–0.3% of the background mixing ratio), superimposed on the more dramatic anthropogenically-driven trend, can be detected (Nevison et al., 2004; 2007; Jiang et al., 2007). However, recent top-down approaches (i.e., atmospheric inversions) have not attempted to resolve seasonality in N_2O sources, in large part due to uncertainties over the influence of the flux of N_2O-depleted air from the stratosphere on tropospheric abundances (Hirsch et al., 2006; Huang et al., 2008).

In this paper, we examine the causes of seasonal variability in atmospheric N_2O at a range of surface monitoring sites, using data from four different monitoring networks. Our primary goal is to assess whether seasonal variations in the N_2O mixing ratio are dominated by biogeochemical signals or by abiotic factors that provide little direct information about surface sources. Our approach is based on efforts to correlate interannual variability in the N_2O seasonal cycle to proxies for known or expected source/sink influences. We deliberately focus on data analysis alone due to concerns that current atmospheric chemical transport models may not accurately capture the biogeochemical source and sink influences that control the N_2O seasonal cycle. A secondary goal is to evaluate whether N_2O seasonal cycles, and interannual variability in those cycles, derived from different monitoring networks are comparable, since an understanding of this question is important for interpreting our results. We focus in particular on sites in the Southern Hemisphere, where the impact of the stratospheric influx of N_2O-depleted air is most uncertain, sites where more than one monitoring network is present, and sites that have contemporaneous CFC-12 measurements. CFC-12 has a similar lifetime and stratospheric sink to N_2O, but few remaining surface sources. We therefore assume that correlated variability in CFC-12 and N_2O primarily reflects transport and stratospheric influences (Nevison et al., 2004, 2007), although this may not always be true, e.g., for air masses coming off the land in developing countries with active sources of both gases.

2 Methods

2.1 N_2O and CFC-12 data

The longest records of atmospheric N_2O are available from the Advanced Global Atmospheric Gases Experiment (AGAGE) and its predecessors (Prinn et al., 2000) and the NOAA Halocarbons and other Atmospheric Trace Species (HATS) (Thompson et al., 2004) networks. Both AGAGE and NOAA/HATS also monitor CFC-12. While both networks began in the late 1970s, the instrumentation has evolved over the years and the high precision data needed to reliably detect seasonal cycles in N_2O are available from the early to mid 1990s for AGAGE and from the late 1990s for NOAA/HATS. The networks include 5 to 6 baseline stations each, making frequent measurements (every ∼40 min) using in situ gas chromatography. The relative precision of the individual AGAGE measurements is about 0.03% (0.1 ppb) for N_2O and slightly less precise for CFC-12. All AGAGE data are measured on the SIO 2005 calibration scale. Monthly mean values are estimated based on the order of 10^3 measurements, with local pollution events removed. Pollution events are defined based on a 2σ deviation from the mean. The NOAA/HATS in situ data are measured using the Chromatograph for Atmospheric Trace Species instruments, abbreviated as CATS. All NOAA data are measured on the NOAA 2006 calibration scale for N_2O and the NOAA 2008 scale for CFC-12.

In addition to the in situ data, the NOAA Carbon Cycle Greenhouse Gases (CCGG) group and the Commonwealth Scientific and Industrial Research Organization (CSIRO) of Australia maintain flask networks, in which duplicate samples are collected every ∼1 to 2 weeks and shipped for analysis on a central gas chromatograph. The CSIRO sites are located primarily in the Southern Hemisphere and date from the early 1990s, while NOAA/CCGG began monitoring N_2O at ∼60 widely distributed flask sampling sites in 1997. The reproducibility of NOAA/CCGG N_2O measurements, based on the mean of absolute values of differences from flask

pairs, is 0.4 ppb. The raw measurement precision for the CSIRO flask N_2O data, which are measured on the CSIRO calibration scale, is estimated as ± 0.3 ppb (Francey et al., 2003). Neither NOAA/CCGG nor CSIRO provides concurrent CFC-12 measurements, however the NOAA/HATS group measures CFC-12 at a subset of the NOAA/CCGG observing sites. Flask and in situ CFC-12 data, if available, are combined in a product referred to as "NOAA/HATS Combined." Table 1 lists the names, code letters, networks, and locations of the sites from which data have been analyzed in this paper.

2.2 Mean seasonal cycles and interannual variability

The N_2O monthly mean data C were detrended by subtracting a 12-month running mean X, centered on month i and calculated independently for each site and network, to remove the long-term trend and other low frequency variability (Eq. 1).

$$X_i = \left(C_{i-6} + 2 \sum_{k=i-5}^{i+5} C_k + C_{i+6} \right) / 24 \quad (1)$$

The remaining high frequency residuals ($C_i - X_i$) were sorted by month and regressed against several proxies, described below, on a month by month basis in an effort to identify causes of interannual variability in the N_2O seasonal cycle. Some sites had gaps in the monthly mean record, which were filled using a 3rd order polynomial fit as a placeholder in the 12-month centered running mean. These filled gaps were not included as data points in the regressions or mean seasonal cycle calculations. Filling the gaps with a higher order polynomial fit had little to no effect on the regression slopes or correlation coefficients. A "mean" seasonal cycle was calculated by taking the average of the detrended data for all Januaries, Februaries, etc.

2.3 Proxies and indices

The detrended monthly means, sorted by month, were regressed against mean polar (60°–90°) lower stratospheric temperature at 100 hPa in winter/spring (January–March in the Northern Hemisphere, September–November in the Southern Hemisphere) from NCEP reanalyses (P. Newman, personal communication, 2009), a proxy for the strength of downwelling of N_2O- and CFC-depleted air into the lower stratosphere (Nevison et al., 2007). For the Southern Hemisphere regressions, temperature data from the previous year, relative to that of the N_2O data, were used in the regressions for January–August, since the effect of the austral winter stratospheric downwelling was not expected to be felt in the troposphere until September at earliest. Regressions also were performed between the detrended N_2O data and the polar vortex break-up date, in both hemispheres, calculated from the method used in Nash et al. (1996) from NOAA/DOE Reanalysis-2 data at 450 K (E. Nash, personal communication, 2009). For the Trinidad Head, California site, the detrended N_2O data were regressed against the NOAA Pacific Fisheries Environmental Laboratory (PFEL) coastal upwelling index (http://www.pfeg.noaa.gov), which is compiled for every 3° of latitude along the Pacific Northwest coastline. For Southern Hemisphere sites, the N_2O data were regressed against the Antarctic Oscillation (http://www.cpc.ncep.noaa.gov), closely related to the Souther Annual Mode (SAM) used as an index of Southern Ocean upwelling (Lovenduski et al., 2007). For all regressions of detrended N_2O monthly means against the proxies described above, the statistical significance of the monthly correlation coefficients was assessed by comparing the calculated R values to critical R values determined from a t-table as a function of $N-2$ degrees of freedom (see Box 15.3 of Sokal and Rohlf, 1981).

2.4 Thermal signals

Atmospheric signals due to seasonal ingassing and outgassing associated with the changing solubility of cooling and warming ocean waters were estimated for N_2O and CFC-12. These were calculated from a simulation of the MATCH atmospheric transport model (Mahowald et al., 1997) forced with a mean annual cycle of thermal O_2 fluxes calculated based on NCEP heat fluxes (Kalnay et al., 1996) and the formula of Jin et al. (2007). The thermal cycles of N_2O and CFC-12 were estimated from the modeled O_2 thermal cycles by scaling by the ratio of the temperature derivative of the respective solubility coefficients (Nevison et al., 2005). The thermal signal in N_2O is uncertain by $\pm \sim 1$ month in phase and $\pm \sim 30\%$ in amplitude (Nevison et al., 2011).

3 Results

3.1 Mean annual cycles

The seasonal cycles in N_2O are small, with mean amplitudes ranging from about 0.3 to 0.9 ppb (Table 1), which amounts to only ~0.1 to 0.3% of the mean tropospheric mixing ratio of 320 ppb. The late summer minima observed in surface N_2O at MHD, BRW (Figs. 1a and S1 in the Supplement) and many other Northern Hemisphere sites (Jiang et al., 2007) appear inconsistent with known biogeochemical N_2O sources, since these alone, apart from abiotic influences, should yield summertime maxima in atmospheric N_2O (Bouwman and Taylor, 1996). Furthermore, the late summer minima are also observed in atmospheric CFC-12, suggesting that common abiotic mechanisms control the seasonality of both species (Nevison et al., 2004, 2007).

The late summer minima, in contrast, appear to be consistent with a stratospheric signal in which air depleted in both N_2O and CFC-12 descends from the middle and upper stratosphere during winter due to the Brewer-Dobson circulation, crosses the tropopause and propagates down to the lower troposphere with a delay of about 3 months (Holton et al., 1995;

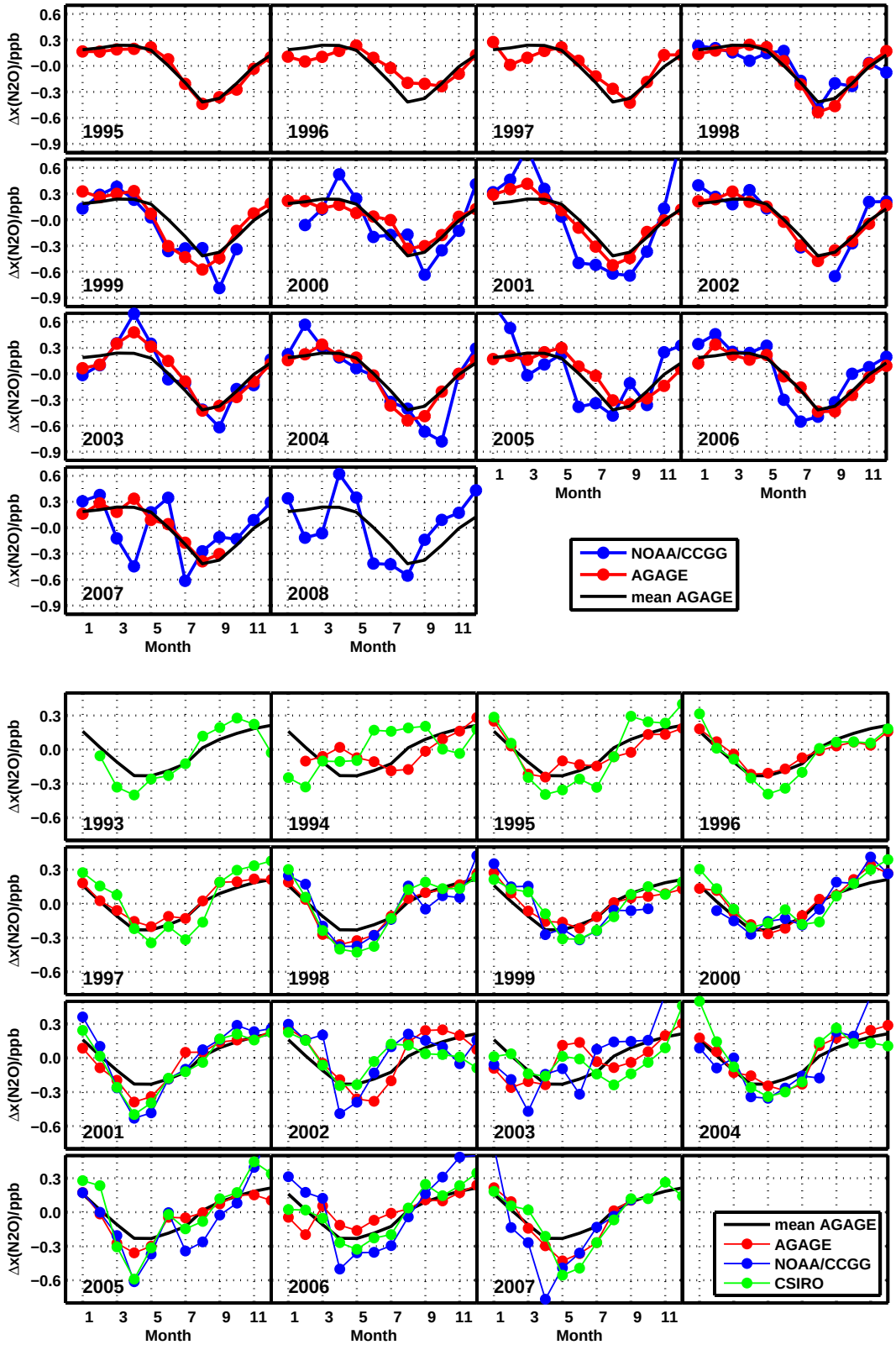

Fig. 1. **(a)** Monthly mean detrended N_2O residuals from AGAGE and NOAA/CCGG networks at Mace Head, Ireland. **(b)** Monthly mean detrended N_2O residuals from AGAGE, NOAA/CCGG and CSIRO networks at Cape Grim, Tasmania.

Table 1. Correlations between N_2O seasonal minimum anomalies and mean polar (60°–90°) lower stratospheric (at 100 hPa) temperature for January–March (Northern Hemisphere) or September–November (Southern Hemisphere). Bold type in final column indicates statistically significant correlations ($p \leq 0.05$).

Site							Mean Seasonal Cycle		Correlation with Stratospheric Temperature		
	Name	Latitude	Longitude	Network[1]	Species	Starting Date	Month of Minimum	Amplitude (ppb)	Month of best anti-correlation	Slope ppb K^{-1} (% error)	R
ALT	Alert, Greenland	82.4	−62.5	N/CCGG	N_2O	Jul 1997	Sep	0.69	Nov	−0.070 (27)	**0.79**
ALT				CSIRO	N_2O	Jul 1992	Sep	0.81	Oct	−0.032 (33)	**0.64**
BRW	Barrow, Alaska	71.3	−156.5	N/CCGG	N_2O	Jan 1998	Aug	0.87	Sep	−0.040 (43)	**0.62**
BRW				N/CATS	N_2O	Jun 1998	Aug	0.93	Aug	−0.043 (39)	**0.67**
BRW				N/CATS	CFC-12	Jun 1998	Sep	0.88[2]	Sep	−0.062[2] (38)	**0.66**
BRW				N/HATS combined	CFC-12	Jan 1990	Sep	1.1[2]	Sep	−0.044[2] (49)	**0.46**
MHD	Mace Head, Ireland	53.3	−9.9	AGAGE	N_2O	Mar 1994	Aug	0.66	Aug	−0.032 (17)	**0.87**
MHD				AGAGE	CFC-12	Mar 1994	Aug	0.89[2]	Aug	−0.045[2] (12)	**0.92**
MHD				N/CCGG	N_2O	Jan 1998	Aug	0.82	Aug	−0.025 (64)	0.48
THD	Trinidad Head, California	40.0	−124.2	AGAGE	N_2O	Oct 1995	Sep	0.32	Jun	−0.019 (58)	0.48
THD				AGAGE	CFC-12	Oct 1995	Aug	0.61[2]	Aug	−0.047[2] (25)	**0.79**
CGO	Cape Grim, Tasmania	−40.7	144.7	AGAGE	N_2O	Aug 1993	May	0.44	Feb	−0.030 (17)	**0.86**
CGO				AGAGE	CFC-12	Aug 1993	Apr	0.44[2]	Feb	−0.025[2] (34)	**0.65**
CGO				N/CCGG	N_2O	Apr 1997	Apr	0.76	Jan	−0.034 (32)	**0.77**
CGO				CSIRO	N_2O	Aug 1992	May	0.55	Mar	−0.016 (70)	0.41
CRZ	Crozet Island	−46.4	51.8	N/CCGG	N_2O	Mar 1997	Apr	0.72	Feb	−0.039 (38)	**0.68**
TDF	Tierra del Fuego	−54.5	−68.5	N/CCGG	N_2O	Jun 1997	May	0.78	Feb	−0.038 (29)	**0.77**
MQA	Macquarie Island	−54.5	159.0	CSIRO	N_2O	Mar 1992	May	0.56	May	−0.068 (25)	**0.75**
PSA	Palmer Station	−64.9	−64.0	N/CCGG	N_2O	Apr 1997	May	0.86	Mar	−0.027 (33)	**0.73**
CYA	Casey Station	−66.3	110.5	CSIRO	N_2O	Nov 96	May	0.67	Apr	−0.023 (54)	0.55
MAA	Mawson	−67.6	62.9	CSIRO	N_2O	Mar 1992	May	0.43	Mar	−0.019 (85)	0.31

Table 1. Continued.

Site							Mean Seasonal Cycle		Correlation with Stratospheric Temperature		
	Name	Latitude	Longitude	Network[1]	Species	Starting Date	Month of Minimum	Amplitude (ppb)	Month of best anti-correlation	Slope ppb K^{-1} (% error)	R
SYO	Syowa	−69.0	39.6	N/CCGG	N_2O	Dec 1995	Jun	0.80	Jan	−0.032 (42)	**0.67**
HBA	Halley Bay	−75.6	−26.4	N/CCGG	N_2O	Feb 1996	Apr	0.81	Mar	−0.025 (42)	**0.62**
SPO	South Pole	−90.0	−26.5	N/CCGG	N_2O	Jan 1997	May	0.75	Mar	−0.021 (64)	0.48
SPO				CSIRO	N_2O	Jan 1992	May	0.65	Mar	−0.018 (65)	0.39
SPO				N/CATS	N_2O	Feb 1998	May	0.53	Feb	−0.011 (73)	0.46
SPO				N/CATS	CFC-12	Mar 1998	Apr	0.57[2]	Feb	−0.044[2] (75)	0.49

[1]NOAA/CCGG, NOAA/HATS and NOAA/CATS abbreviated as N/CCGG, N/HATS and N/CATS.

[2]CFC-12 slopes and mean seasonal amplitudes are normalized to N_2O units by multiplying by the ratio of the mean tropospheric mixing ratios $x(N_2O)/x$(CFC-12), where $x(N_2O)$ is in ppb and x(CFC-12) is in ppt.

Nevison et al., 2004; Liang et al., 2008, 2009). The stratospheric hypothesis is somewhat controversial, in part because the observed seasonal cycles in N_2O may also reflect purely tropospheric transport mechanisms, e.g., summer vs. winter differences in convection and boundary layer thickness, especially at northern high latitudes. However, past modeling studies generally have not been able to reproduce observed surface seasonal cycles in N_2O and CFC-12 in the Northern Hemisphere based on surface sources and tropospheric transport alone (Nevison et al., 2007; Liang et al., 2008).

In the Southern Hemisphere, N_2O and CFC-12 have similar seasonal cycles at Samoa and Cape Grim, Tasmania, again suggesting common abiotic influences (Nevison et al., 2004, 2007). Seasonal changes in interhemispheric transport likely dominate the seasonal cycles at tropical Samoa, but do not appear to explain the fall minima in N_2O and CFC-12 observed at extratropical southern sites (Figs. 1 and S2 in the Supplement, Table 1) (Nevison et al., 2007; Liang et al., 2008). Ishijima et al. (2010) found good agreement with the observed atmospheric N_2O sesaonal cycle at Cape Grim, Tasmania using the seasonal oceanic source of Nevison et al. (1995) in a transport model simulation, with little to no contribution from stratospheric or tropospheric transport influences. However, Nevison et al. (1995) probably substantially overestimated the actual Southern Ocean N_2O source (Nevison et al., 2005).

A third abiotic influence on atmospheric N_2O data is the thermal signal due to changing solubility in warming and cooling surface ocean waters. The thermal signal is maximum in late summer in both hemispheres. It tends to oppose the observed seasonal cycle at most sites, although not at THD (Fig. 2), and thus cannot by itself explain the observed cycle.

3.2 Interannual variability and differences among monitoring networks

N_2O data display considerable interannual variability, such that the concept of a "mean" seasonal cycle may not be very meaningful at some sites (e.g., Fig. 2). In addition, different monitoring networks that share common sites sometimes observe seasonal cycles that differ substantially in both shape and amplitude (e.g., Figs. 1a,b and S1, S2 in the Supplement, Table 1). Some of the variability among networks may reflect local meteorology at the time of sampling or data filtering. To evaluate this possibility, we examined, for each month of the seasonal cycle, whether the detrended N_2O monthly means from different networks that share a common site show correlated interannual variability, e.g., whether an unusually deep August minimum in a given year observed by a given network is also observed for that year by other networks. At Mace Head, which is sampled by both the in situ AGAGE network and the NOAA/CCGG flask network, the detrended, pollution-filtered AGAGE data (Fig. 1a) are significantly correlated to the NOAA/CCGG data in February, but not for any other month. At Cape Grim, which is sampled by AGAGE, NOAA/CCGG and the CSIRO flask network (Fig. 1b), the detrended N_2O monthly means are significantly correlated among the three networks in ∼March–May, around the time of the seasonal minimum, with R values around 0.7. At

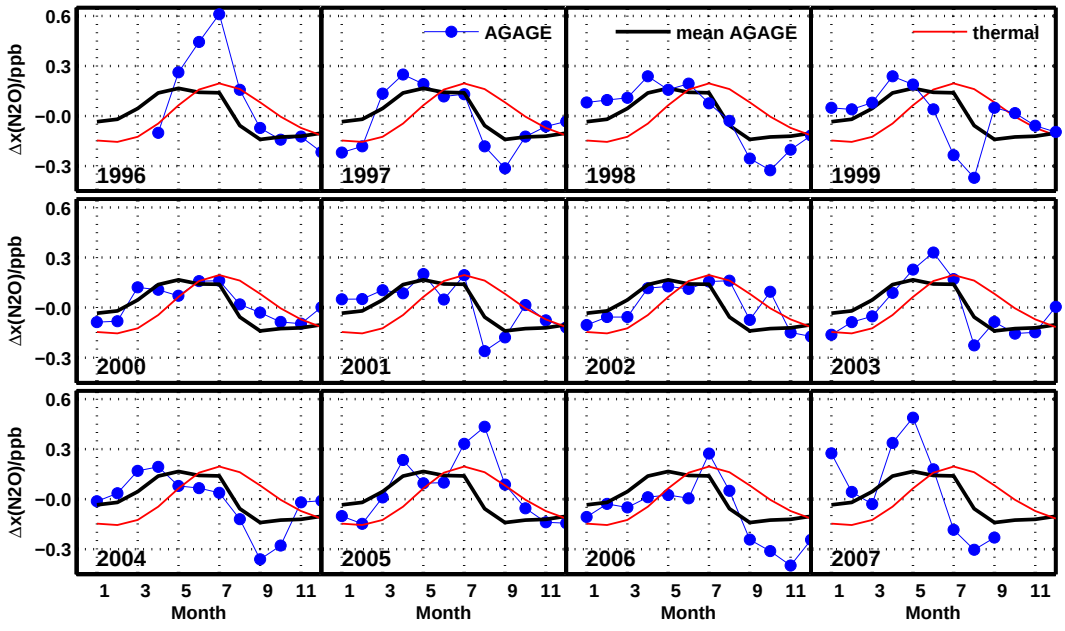

Fig. 2. Monthly mean detrended AGAGE N_2O residuals at Trinidad Head, California. The "mean" annual cycle in observed N_2O and estimated mean annual thermal N_2O cycle associated with oceanic ingassing and outgassing are superimposed on each year's observed cycle.

Barrow, Alaska, the detrended N_2O monthly means are not significantly correlated between NOAA/CCGG and in situ CATS data (Fig. S1 in the Supplement). At South Pole, the detrended N_2O data are weakly correlated around the time of the May seasonal minimum among the NOAA/CATS, NOAA/CCGG and CSIRO networks, with R values only around 0.5 (Fig. S2 in the Supplement).

The general lack of correlation in detrended N_2O data between NOAA/CCGG and the AGAGE and NOAA/CATS networks at Mace Head and Barrow, respectively, could reflect limitations specific to NOAA/CCGG data. Alternatively, it could reflect the fact that interannual variability in the N_2O seasonal cycle at northern sites is more strongly influenced by local conditions, including meteorology and pollution events, and data filtering artifacts than at southern sites. At MHD, about 20% of the in situ AGAGE measurements are tagged as pollution events compare to only 5% at CGO. When AGAGE data are subsampled at MHD at the time of NOAA/CCGG flask collection, the subsampled dataset picks up a number of somewhat erratic features that show up in the NOAA/CCGG data, but that are smoothed out or tagged as pollution events in the full AGAGE dataset (Fig. 3a and b). At CGO, subsampling of the AGAGE data at the time of NOAA/CCGG or CSIRO flask collection can explain some of the differences between the full AGAGE dataset and the two flask networks, but does not appear to be the only factor governing the discrepancies among the networks (Fig. 4). In general, detecting subtle seasonal and interannual signals in N_2O data is more difficult for a flask network sampling every 1–2 weeks, with an average flask pair agreement of 0.4 ppb (in the case of NOAA/CCGG), than for an in situ network with a high-frequency measurement record. While NOAA/CCGG employs a pollution-filtering algorithm similar to that of AGAGE, based on 2 to 3σ deviations from the mean, it is generally less able to screen out pollution events, due to lower frequency of data. The two networks conduct regular, twice yearly comparisons at common sites, but the focus is on absolute tropospheric mixing ratios rather than on seasonal and interannual variability.

3.3 Causes of interannual variability in the seasonal cycle

3.3.1 Northern Hemisphere

In an effort to understand the causes of N_2O seasonality, we compared interannual variability in the seasonal cycle to several proxies that offer mechanistic insight. The first of these proxies is mean winter polar lower stratospheric temperature, which varies year to year with the strength of the Brewer-Dobson circulation, with warmer temperatures reflecting stronger circulation. We find striking correlations between the stratospheric temperature proxy and the detrended AGAGE N_2O monthly means at MHD from Fig. 1a, sorted by month, particularly in July–September, the months surrounding the August minimum (Figs. 5 and 6). Similar correlations are observed between stratospheric temperature and

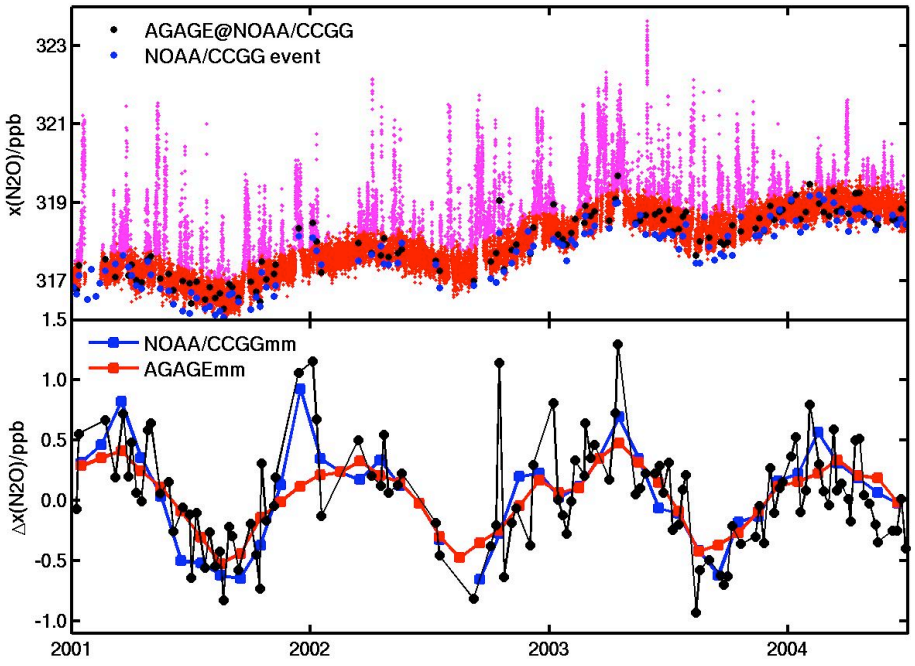

Fig. 3. **(a)** N_2O data at Mace Head, Ireland from January 2001–June 2004. Warm colors show complete AGAGE in situ data. Magenta indicates data tagged as pollution events. Blue dots are NOAA/CCGG event (i.e., weekly flask) data. Black circles are AGAGE data subsampled at the time of NOAA/CCGG flask collection. **(b)** AGAGE data subsampled at the time of NOAA/CCGG flask collection. Solid squares show the monthly mean data for AGAGE and NOAA/CCGG. All data have been detrended with a 12-month centered running mean of their respective networks.

detrended MHD CFC-12 monthly means around the August seasonal minimum (Fig. 7). The sign of the correlations is such that deeper (more negative) surface N_2O and CFC summer minima occur during warm years, in which stronger than average descent of air depleted in N_2O and CFC-12 occurs into the polar lower stratosphere during winter. The regressions yield slopes, N_2O/CFC-12 in ppb/K/(ppb/K), with a ratio of about 0.7 (where CFC-12 has been normalized to N_2O units by multiplying by $[x(N_2O)/ppb]/[x(CFC\text{-}12)/ppt]$. The NOAA/CATS data at BRW give a similar slope ratio. The 0.7 ratio is notably similar to the Volk et al. (1997) slope of normalized N_2O vs. CFC-12 data measured near the tropopause.

In addition to the AGAGE correlations at MHD, Fig. 7 and Table 1 show statistically significant correlations between mean winter polar lower stratospheric temperature and the detrended N_2O seasonal minima at ALT for both CSIRO and NOAA/CCGG data and at BRW for both NOAA/CATS and NOAA/CCGG data. Significant correlations also are observed between stratospheric temperature and detrended CFC-12 seasonal minima at THD for AGAGE and at BRW, both for NOAA/CATS in situ data and for NOAA/HATS combined in situ/flask data, for time series beginning in the 1990s and extending through the present. For the northern sites in Fig. 7 and Table 1, the strongest correlation with stratospheric temperature typically occurs during the month of the N_2O or CFC-12 minimum (August or September) or shortly after.

At MHD, NOAA/CCGG detrended N_2O minima show a weak, although not statistically significant, correlation with stratospheric temperature (Fig. 7b). Figure 3b suggests that the difference between the AGAGE and NOAA/CCGG results at MHD may be a sampling issue, in which the relatively infrequent weekly NOAA/CCGG flask samples intersect with pollution influences and noise due to atmospheric variability in the N_2O data to obscure subtle interannual signals. In support of this hypothesis, the AGAGE N_2O data at MHD are themselves only weakly correlated with stratospheric temperature when pollution-filtered monthly means are replaced with unfiltered data, with the R values for the detrended August monthly means dropping from 0.87 to 0.49.

A month-by-month summary of the correlations between stratospheric temperature and detrended AGAGE N_2O data at MHD shows that, in addition to the negative summertime correlations around the time of the seasonal minimum, significant positive correlations with stratospheric temperature occur in February–March near the time of the N_2O maximum (Fig. 6). These correlations (which also are seen in AGAGE CFC-12 data at MHD and THD, and are apparent to varying degrees but generally not statistically significant at other northern N_2O monitoring sites) reflect the fact that the overall amplitude of the N_2O seasonal cycle is

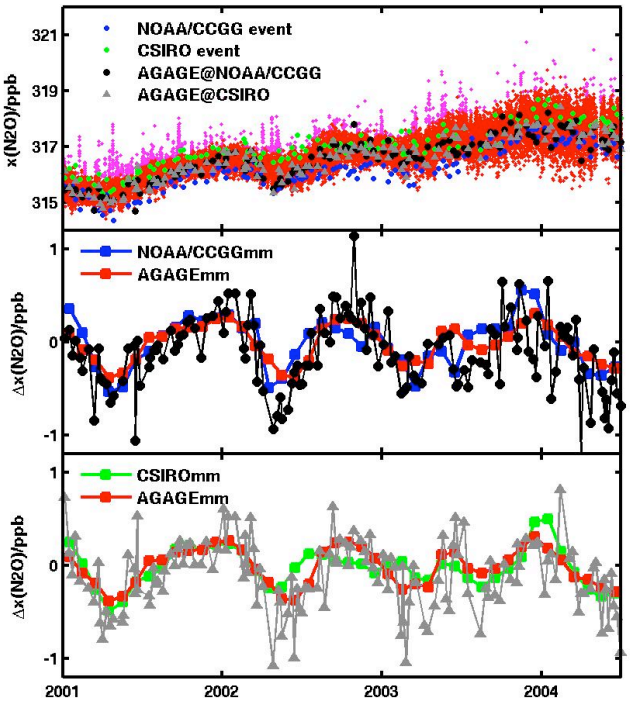

Fig. 4. **(a)** Same as Fig. 3a but for Cape Grim,Tasmania. Green dots are CSIRO event data. Gray triangles are AGAGE data subsampled at the time of CSIRO flask collection. **(b)** AGAGE data subsampled at NOAA/CCGG flask times compared to AGAGE and NOAA/CCGG monthly means. **(c)** AGAGE data subsampled at CSIRO flask times compared to AGAGE and CSIRO monthly means. All data in **(b)** and **(c)** have been detrended as described in Fig. 3b.

strongly correlated to stratospheric temperature ($R = 0.92$), with larger amplitudes in warm years. To further understand these correlations, we note that the N_2O seasonal cycle at MHD is more strongly characterized by its minimum than by its maximum and that the onset of descent into the minimum is a more distinct feature of the data than the month of the actual maximum (Figs. 1a and S3 in the Supplement). Notably, the month of onset of descent into the summer minimum at MHD is itself correlated to stratospheric temperature ($R = 0.90$, see Fig. S3 in the Supplement), with earlier onset of descent occurring in warm years.

The February–March positive correlations are also to some extent a function of the centered, 12-month running mean used to detrend the N_2O data (Eq. 1), which tends to bisect the N_2O seasonal cycle each year (Fig. S4 in the Supplement), leading to larger maxima in warm years, when the overall amplitude of the cycle is larger. In addition, the running mean reflects the atmospheric growth rate in N_2O, which itself is correlated to polar lower stratospheric temperature at MHD, with slower growth occurring in warm years (Nevison et al., 2007). The result is a flatter curve being subtracted from the raw monthly mean N_2O data in warm years, which tends to increase the February–March residuals used in our regressions. Figures S3–S5 in the Supplement provide a more detailed examination of the relationship between the month of onset of descent into the seasonal N_2O minimum at MHD as well as the sensitivity of the regressions to our detrending methodology.

We assert that the most likely interpretation of the correlations with stratospheric temperature discussed above is a strong and coherent stratospheric influence on the seasonal cycles of surface N_2O and CFC-12 observed at Northern Hemisphere monitoring sites. While alternative hypotheses are possible, e.g., that the correlations arise because tropospheric N_2O variability is driven by weather anomalies, e.g., in convection over continents, that in turn correlate with stratospheric temperatures, model evidence suggests that the observed correlations are more consistent with a direct stratospheric influence (see Figs. S6–S8 in the Supplement). Section 4 discusses the likely mechanistic pathway responsible for the correlations.

Trinidad Head, California is an interesting case in which the detrended AGAGE CFC-12 monthly means are significantly correlated to stratospheric temperature in August, but the detrended AGAGE N_2O monthly means are not (Fig. 8a and c). Since N_2O data at THD are known to be influenced by ventilation of N_2O-enriched deepwater during coastal upwelling events (Lueker et al., 2003), we performed additional regressions of detrended THD N_2O data against the coastal upwelling index for the Pacific Northwest. Correlations of $R = 0.45$ to 0.66 were found in April–September (the upwelling season), with more positive N_2O values occurring during years of strong upwelling (Fig. 8b). A multivariate regression of detrended N_2O data against the upwelling index and stratospheric temperature improved these correlations to $R = 0.64$ to 0.82 for April–September (Fig. 8d). Statistically significant correlations were obtained from the multivariate regression using the coastal upwelling indices at 42° N, 45° N and 48° N (THD is at 40° N), with best results obtained for the 45° N index. Figure S9 in the Supplement provides more details on the THD regressions.

3.3.2 Southern Hemisphere

The Brewer-Dobson circulation is thought to be weaker in the Southern Hemisphere, with descent into the winter pole that is less strongly seasonal than in the Northern Hemisphere (Table 1 in Holton et al., 1995). Accordingly, the stratospheric influence on N_2O and CFC-12 has been less clear in previous model studies in the Southern Hemisphere. Two atmospheric general circulation-based chemical transport models, the Whole Atmosphere Community Climate Model (WACCM) and the Research Institute for Global Change/JAMSTEC ACTM model did not produce a stratospheric signal in N_2O (or in CFC-12 for WACCM) at surface sites in the Southern Hemisphere, although both models predicted a coherent signal in summer in the Northern

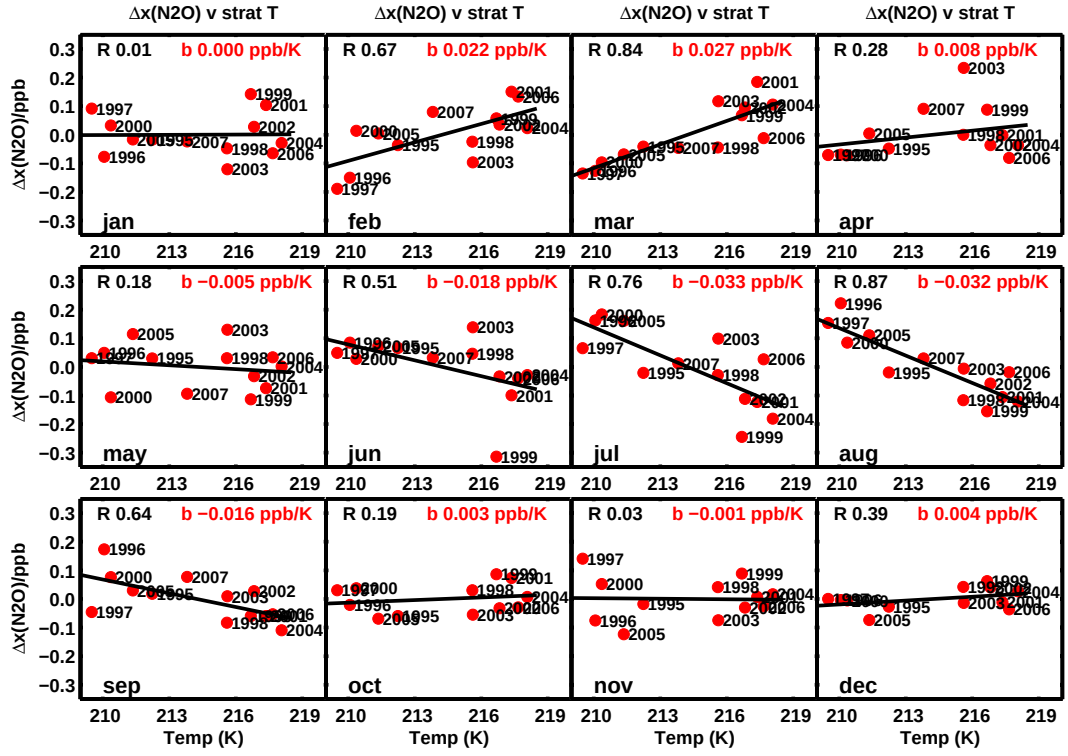

Fig. 5. Detrended AGAGE N_2O data at Mace Head, Ireland (from Fig. 1a), sorted by month and plotted vs. mean polar (60–90° N) winter (January–March) lower stratospheric (100 hPa) temperature from NCEP reanalysis data. The mean of the detrended N_2O data for each month is subtracted to permit all months to be plotted with the same y-axis scale. The Pearson's correlation coefficient R and the slope b of each linear regression are shown.

Hemisphere (Nevison et al., 2004; Ishijima et al., 2010). In contrast, the GEOS CCM model found coherent cycles in CFC-12 with autumn minima, in good agreement with observations (Liang et al., 2008).

Due to the conflicting results of previous model studies, we take an observational approach here, regressing detrended month meanly N_2O and CFC-12 data, sorted by month, against mean 60–90° S September–November temperature in the lower stratosphere from the previous spring. We use spring temperature, rather than winter temperature as for the Northern Hemisphere, because the polar vortex is more stable and persistent in the Southern Hemisphere. Vortex breakup typically occurs in November–December (compared to March–April in the Northern Hemisphere) (Waugh et al., 1999), which allows cold temperatures and depleted levels of N_2O and CFC-12 to persist into late spring. In Fig. 9, the detrended AGAGE N_2O monthly means in January–February at Cape Grim show statistically significant anticorrelations with stratospheric temperature, with more negative values occurring during warm years. By May–June, however, the detrended N_2O data become positively correlated to stratospheric temperature (Fig. 9). The summary plot of the CGO correlations with stratospheric temperature shows that, unlike in the Northern Hemisphere, the strongest negative correlations are found several months before the seasonal minimum and that positive correlations are observed at and shortly after the month of the seasonal minimum. Similar correlation patterns with stratospheric temperature are found for AGAGE CFC-12 (Fig. 10a).

The NOAA/CCGG flask data at CGO show correlation patterns with stratospheric temperature similar to those seen by AGAGE, although the correlations are statistically significant only in January (Fig. 10d). In addition, both the NOAA/CCGG and CSIRO flask networks show correlation patterns similar to those seen at CGO by AGAGE at many of their other extratropical southern sites (Fig. 11, Table 1). In most cases, the anticorrelations are strongest in the months preceding the N_2O minimum, which typically occurs in May, with the exception of Macquarie Island, where the anticorrelation is strongest in May. At South Pole, neither the CSIRO, CATS nor NOAA/CCGG networks shows statistically significant correlations between detrended N_2O data and stratospheric temperature.

In an effort to better understand the above findings, and because the N_2O minimum at southern sites varies from January–June in individual years, most commonly occuring in April or May, we regressed the month of the AGAGE N_2O minimum at CGO against both polar lower stratospheric

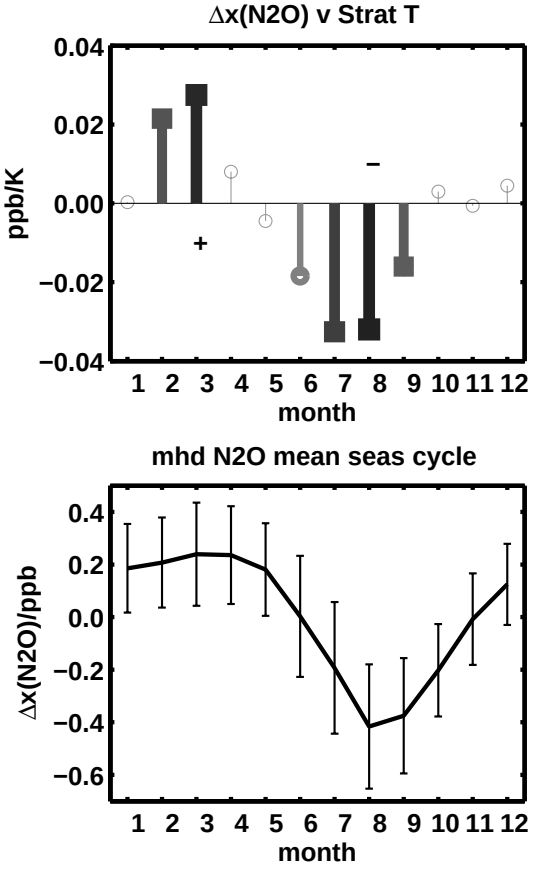

Fig. 6. **(a)** Stem plot summarizing the correlation slopes between AGAGE detrended N_2O monthly means at Mace Head and northern polar winter lower stratospheric temperature from Fig. 5. Heavy lines indicate statistically significant correlations. The darker the line, the higher the R value. Negative slopes in July–September indicate deeper minima at warmer stratospheric temperature, **(b)** "mean" seasonal cycle at Mace Head for AGAGE N_2O, with error bars showing the standard deviation for each month.

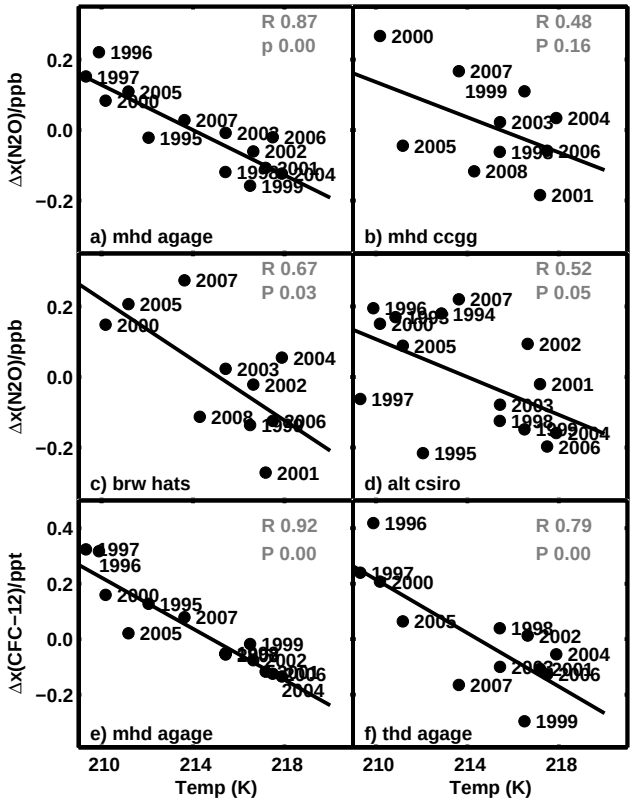

Fig. 7. Detrended N_2O residuals at the minimum month in the mean annual cycle (September for Alert, August for the other sites) vs. polar winter lower stratospheric temperature, N_2O **(a–d)** and CFC-12 **(e–f)** data are from AGAGE, NOAA/HATS, NOAA/CCGG or CSIRO monitoring sites as indicated on the panels. The Pearson's correlation coefficient R and the p value based on a Student's t distribution for each linear regression are shown, where a value of $p \leq 0.05$ is statistically significant (Sokal and Rohlf, 1981).

temperature and polar vortex break-up date and found that earlier minima tended to occur in years with warm temperatures ($R = 0.75$) and early vortex break-up ($R = 0.62$) and later minima in years with cold temperatures and late vortex break-up. Similar but stronger correlations were found between the N_2O maximum at CGO (defined as the onset of descent into the minimum) and both stratospheric temperature ($R = 0.92$) and vortex break-up date ($R = 0.90$). These correlations are widespread in N_2O data at other Southern Hemisphere sites, although generally less statistically significant than in AGAGE N_2O data at CGO. We note also that vortex break-up date and polar lower stratospheric temperature are themselves correlated in both hemispheres (Waugh et al., 1999) ($R = 0.79$ for the Southern Hemisphere vortex break-up and temperature indices used here), with later vortex break-up occurring during cold years. Figures S10 and S11 in the Supplement provide more details on the timing of the AGAGE N_2O minima and maxima at CGO and their correlation to stratospheric temperature and vortex break-up date.

Coupled ocean biogeochemistry-atmospheric transport model simulations suggest that N_2O monitoring sites in the Southern Ocean region are influenced by ventilation of oceanic, microbially-produced N_2O (Jin and Gruber, 2003; Nevison et al., 2005). This is especially true of sites situated in the heart of the Antarctic Circumpolar Current (Orsi et al., 1995), between ∼50°–60° S, where strong winds and upwelling lead to deep ventilation of N_2O-enriched subsurface waters. Following the example discussed for the northern THD site, which is influenced by coastal upwelling, we regressed detrended N_2O monthly mean flask data at the Southern Hemisphere sites in Table 1 against a multivariate combination of stratospheric temperature and the Southern Annular Mode index, a proxy for Southern Ocean upwelling (Lovenduski et al., 2007). However, we did not find any statistically significant correlations beyond those already discussed above for stratospheric temperature alone.

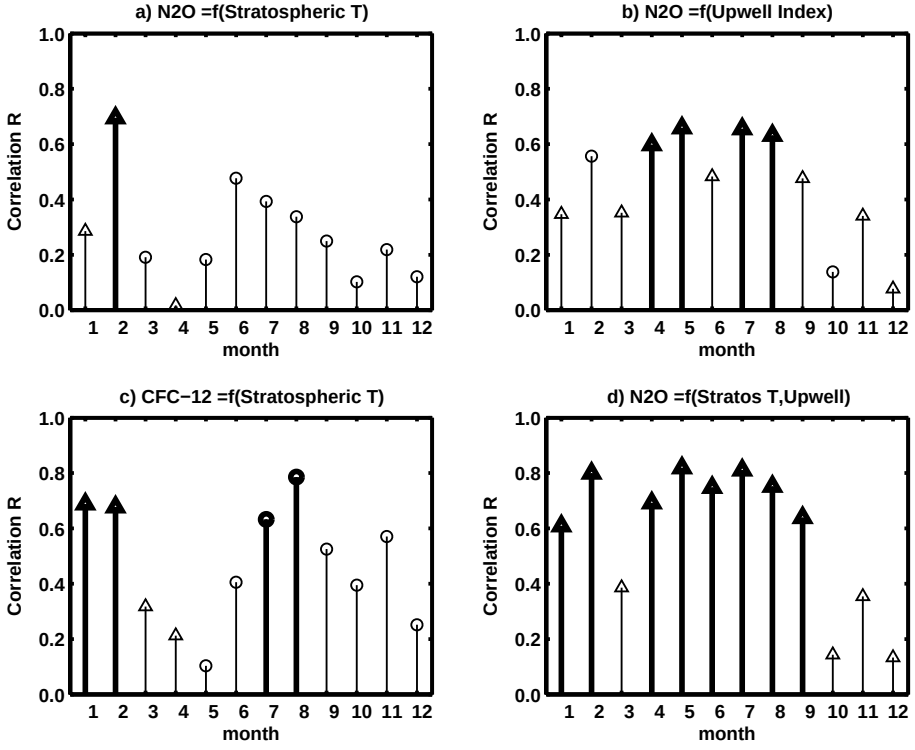

Fig. 8. Stem plots summarizing the linear regression slopes for detrended AGAGE N_2O or CFC-12 monthly means at Trinidad Head vs. polar winter lower stratospheric temperature and/or the NOAA PFEL upwelling index for the Oregon coast at 45° N. Heavy black lines indicate statistically significant correlations. Triangles indicate a positive correlation, circles indicate a negative correlation – e.g., in panel **(c)**, warmer stratospheric temperatures are correlated to more negative CFC-12 values in July–August, i.e., deeper seasonal minima. **(a)** N_2O vs. stratospheric temperature, **(b)** N_2O vs. upwelling index, **(c)** CFC-12 vs. stratospheric temperature, **(d)** multivariate regression of N_2O vs. stratospheric temperature and upwelling index.

Nevison et al. (2005) hypothesized that the N_2O seasonal cycle in the extratropical Southern Hemisphere can be decomposed into more or less comparable contributions from ocean ventilation, the stratospheric influx signal, and an abiotic thermal signal due to warming and cooling of surface waters (Fig. 12a). The stratospheric signal in Fig. 12a is estimated based on the observed, normalized CFC-12 cycle at CGO multiplied by a scaling factor which is uncertain, but which we assign a best guess value of 0.7 based on the discussion in Sect. 3.3.1. Unlike THD, where the thermal signal is in phase with the summer upwelling N_2O source, ventilation of Southern Ocean waters occurs during the breakdown of the seasonal thermocline in fall and winter, and thus opposes the thermal signal. In Fig. 12b, the thermally-corrected N_2O cycle, i.e., subtracting the estimated thermal signal from the observed "mean" seasonal cycle, yields a cycle that closely resembles the observed CFC-12 cycle. (CFC-12 also experiences thermal ingassing and outgassing, but is 8 times less soluble than N_2O, such that the thermal correction has little impact on its cycle – Fig. 12b.) The N_2O ocean ventilation and stratospheric signals are roughly coincident, with the former a positive signal peaking in early fall and the latter a negative signal peaking in spring, making the two signals difficult to distinguish.

4 Discussion

We conclude, based primarily on the strong correlations between polar lower stratospheric temperature and detrended AGAGE N_2O and CFC-12 data at MHD (Figs. 5 and 6) and CGO (Figs. 9 and 10a and c), which provide the longest high-resolution time series of these gases in the Northern and Southern Hemispheres, respectively, that the stratosphere exerts a coherent influence on surface N_2O and CFC-12 seasonal cycles in both hemispheres. The correlations between the phasing of the AGAGE N_2O seasonal cycle at MHD and CGO and both stratospheric temperature and polar vortex break-up date further indicate a stratospheric influence (Figs. S3, S10, and S11 in the Supplement). The results from other networks and sites in the Northern (Fig. 7) and Southern Hemispheres (Figs. 10–11) are generally less compelling, but, in the context of the AGAGE results, provide additional support for the stratospheric hypothesis.

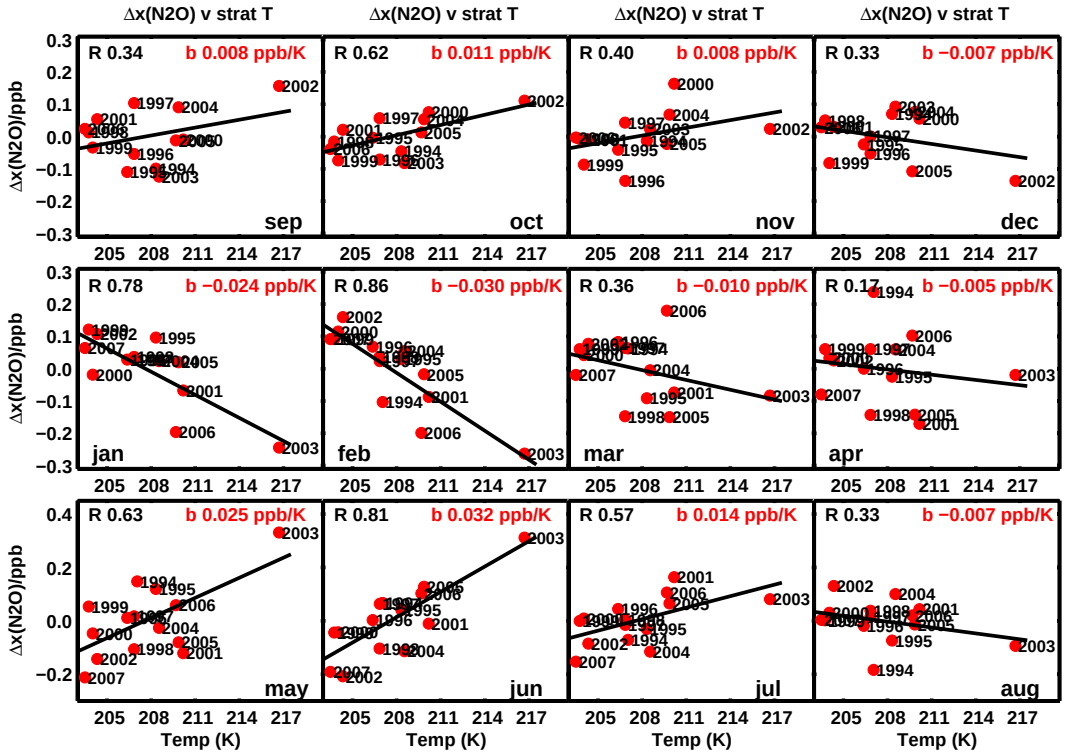

Fig. 9. Detrended AGAGE N_2O data at Cape Grim, Tasmania (from Fig. 1b), sorted by month and plotted vs. mean polar (60–90° S) spring (September–November) lower stratospheric (100 hPa) temperature from NCEP reanalysis data. The mean of the detrended N_2O data for each month is subtracted to permit all months to be plotted on a similar y-axis scale. The Pearson's correlation coefficient R and the slope b of each linear regression are shown. Note that the year labels correspond to the year of the detrended N_2O monthly means, which for January–August are plotted against the previous year's spring (September–November) stratospheric temperature, when cold air is still generally trapped in the polar vortex. A sudden stratospheric warming occurred in September 2002, leading to anomalously warm polar temperatures in the spring lower stratosphere (Glatthor et al., 2005).

The mechanistic pathway between the polar lower stratosphere and the mid-to-high latitude lower troposphere is not obvious, but evidence from stratospheric N_2O observations (e.g., Engel et al., 2006) and model simulations (Liang et al., 2009) points toward an explanation involving a convolution of the phase and amplitude of the N_2O seasonal cycle in the lower stratosphere and the overall mass transport across the tropopause. Brewer-Dobson descent from the middle and upper stratosphere leads to a large seasonal amplitude in N_2O in the polar lower stratosphere, which reaches its minimum in winter or spring, around the time of polar vortex break-up, with gradients of 50 ppb or more with respect to the troposphere. Slow diabatic descent across the polar tropopause brings this N_2O-depleted air into the troposphere, where it undergoes efficient exchange between the mid and high latitudes via various synoptic-scale eddies in extra-tropical cyclones (Stohl, 2001). Air of polar stratospheric origin experiences strong dilution when it enters the troposphere by this pathway. By the time it propagates down to the lower troposphere, on a time scale of ∼3 months, the stratospheric signal is reduced by a factor of ∼100, leading to the <1 ppb seasonal amplitude observed in N_2O at surface sites (Nevison et al., 2004; Liang et al., 2009).

The vertical downward penetration across the tropopause associated with the Brewer-Dobson circulation is slow and inefficient compared to stratosphere-troposphere exchange (STE) in the mid-latitudes, occurring, e.g., via quasi-isentropic horizontal mixing and tropopause folds (Holton et al., 1995). When the polar vortex breaks down in spring (or sometimes early summer in the Southern Hemisphere), N_2O-depleted polar air mixes with mid-latitude air in the lower stratosphere, but dilution accompanies this mixing and the cross-tropopause gradients of N_2O observed at mid-latitudes are considerably smaller than those at the poles (Engel et al., 2006). At present, it is not clear whether strong mid-latitude STE of a weak lower stratospheric signal or weak descent across the polar tropopause of a strong stratospheric signal, or a combination of both, controls the stratospheric influence felt in the troposphere. Time series observations of N_2O in the lower stratosphere from satellites (Lambert et al., 2007; Khosrawi et al., 2008) and altitude-resolved profiles in the troposphere from aircraft (Ishijima et al., 2010; Wofsy et al., 2011) may help shed light on the amplitude and phasing of

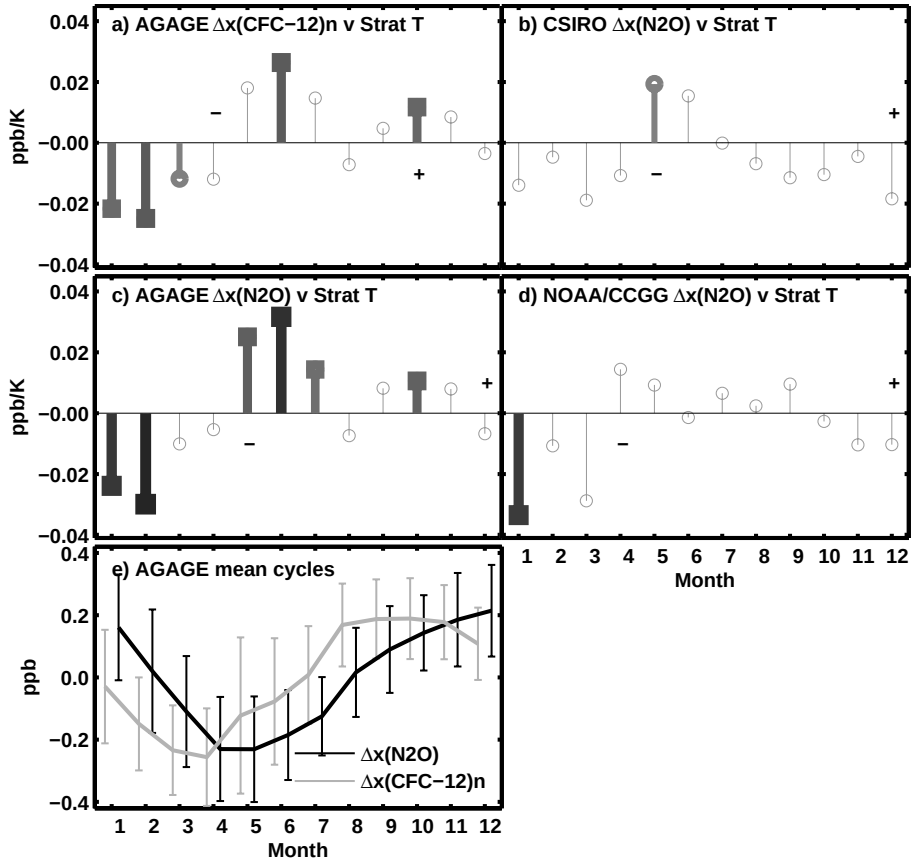

Fig. 10. Stem plots summarizing the linear regression slopes for detrended N_2O or CFC-12 monthly means at Cape Grim vs. mean southern polar spring lower stratospheric temperature. Heavy lines indicate statistically significant correlations. The darker the line, the higher the *R* value: **(a)** AGAGE CFC-12, normalized by [x(N_2O)/ppb]/[x(CFC-12)/ppt] and expressed in ppb units, **(b)** CSIRO N_2O, **(c)** AGAGE N_2O, **(d)** NOAA/CCGG N_2O, **(e)** mean seasonal cycle for AGAGE N_2O and normalized CFC-12, with error bars showing the standard deviation for each month.

the seasonal cycle in N_2O throughout the lower stratosphere and provide a better understanding of the mechanism(s) by which the stratospheric signal propagates down to the lower troposphere.

The correlation coefficients in Fig. 7 and Table 1 between Northern Hemisphere detrended N_2O and CFC-12 minima and polar lower stratospheric temperature indicate that the interannual variability in the stratospheric signal can account for anywhere between ∼75% (at MHD) and ∼25% (at ALT) of the variability in the detrended minima. Noise in the data, biogeochemical sources and tropospheric transport variability, especially at high latitudes, may account for the remainder. Since interannual variability in the strength of the stratospheric influence (represented by the winter polar lower stratospheric temperature proxy) can explain a substantial portion of the interannual variability in the surface N_2O seasonal cycle observed at northern sites, it follows logically that the stratospheric influence is substantially responsible for causing the seasonal cycle in the first place.

Our regressions of detrended monthly mean N_2O data against coastal and open ocean upwelling indices at Trinidad Head, California and Southern Ocean sites, respectively, illustrate some of the challenges involved in identifying biogeochemical signals in tropospheric data that are influenced by stratospheric and other abiotic signals. At THD, located near a strong, natural, regional N_2O source, we found correlations between detrended N_2O data and the NOAA/PFEL coastal upwelling index, but these were more statistically significant after accounting for the stratospheric influence using a multivariate regression. In the Southern Hemisphere, we were unsuccessful at correlating detrended N_2O monthly means to interannual variability in the SAM, an index of Southern Ocean upwelling. The lack of correlation with SAM does not necessarily show that there is no oceanic biological N_2O signal at these sites, but it does suggest that the biological signal is either relatively constant year to year or weaker than the abiotic stratospheric and thermal signals, both of which act to obscure it (Fig. 12).

THD was the only northern site where we applied our regression methodology using a biogeochemical source proxy, since most N_2O sources, both natural and anthropogenic, are not well quantified. The commonly-used source databases

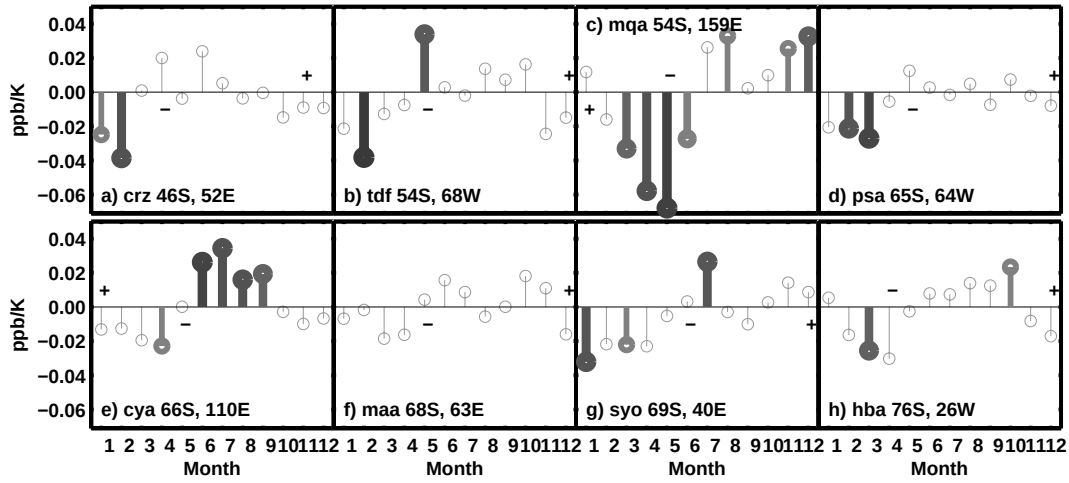

Fig. 11. Stem plots summarizing the linear regression slopes for detrended N_2O monthly means at 8 different Southern Hemisphere sites spanning 3 monitoring networks vs. mean southern polar spring lower stratospheric temperature. Heavy lines indicate statistically significant correlations at the 5% confidence level, with darker lines, signifying higher *R* values. Medium grey lines with open circles indicate marginally significant correlations at 10% confidence level: **(a)** Crozet Island (NOAA/CCGG), **(b)** Tierra del Fuego (NOAA/CCGG), **(c)** Macquarie Island (CSIRO), **(d)** Palmer Station (NOAA/CCGG), **(e)** Casey Station (CSIRO), **(f)** Mawson (CSIRO), **(g)** Syowa (NOAA/CCGG), **(h)** Halley Bay, (NOAA/CCGG).

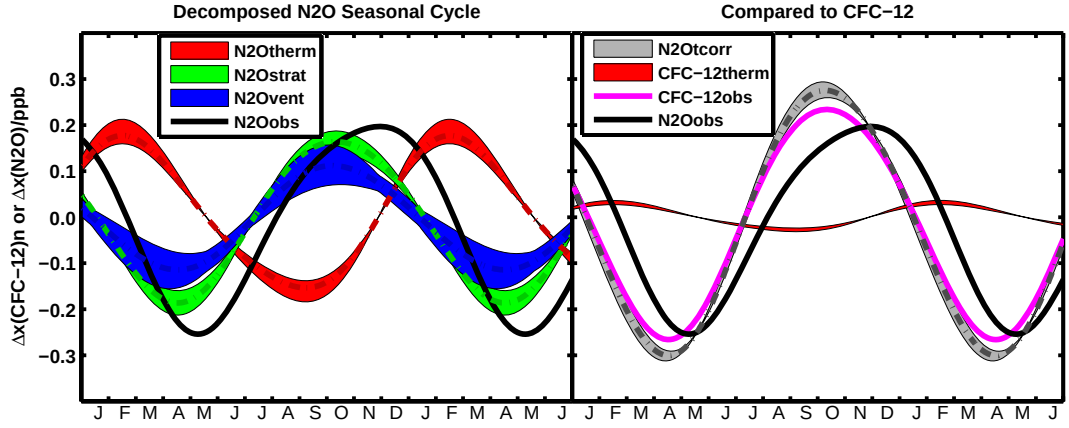

Fig. 12. (a) Decomposition of N_2O seasonal cycle at Cape Grim based on methodology described in Nevison et al. (2005). Envelopes show estimated uncertainty in stratospheric and thermal signals, with the biological oceanic ventilation signal derived as a residual of observed N_2O minus the thermal and stratospheric terms. Figure uses smoothed, idealized curves. **(b)** Comparison of observed CFC-12 seasonal cycle at Cape Grim to the observed N_2O cycle, before and after correcting N_2O for the thermal signal from **(a)**. The corresponding thermal signal in CFC-12 is small (red envelope) and does not substantially change the observed CFC-12 seasonal cycle. The observed and thermal CFC-12 curves are shown in ppb units, after being normalized by $[x(N_2O)/\text{ppb}]/[x(\text{CFC-12})/\text{ppt}]$.

(e.g., EDGAR, Olivier et al., 2005, and GEIA, Bouwman et al., 1995) are uncertain, often providing only annual resolution, and few obvious observationally-based proxies for interannual variability in these sources exist. However, our results at Trinidad Head provide a basis for optimism that high-precision monitoring of atmospheric N_2O at sites located near strong, seasonally-varying anthropogenic sources may help shed light on these sources, especially if due attention is paid to confounding abiotic influences. Some possible examples include polluted coastal regions receiving heavy agricultural nitrogen runoff that are also subject to seasonal upwelling (e.g., Naqvi et al., 2000 or sites located within the Midwestern US agricultural belt, which show interannual variability in the seasonal cycle similar in magnitude to that at THD; http://www.esrl.noaa.gov/gmd/ccgg/iadv/).

Our study reveals some interesting differences between Northern and Southern Hemisphere N_2O seasonal cycles and their correlations with polar lower stratospheric temperature, not all of which have clear explanations. The autumn versus summer minima observed at southern versus northern sites

seem logically related to the longer persistence of the Southern Hemisphere polar vortex, which in theory should result in a later N_2O minimum in the lower stratosphere. The relatively phase-invariant late summer minima observed at northern sites, compared to the more variable minima at southern sites, could reflect a strong contribution from tropospheric transport processes in the Northern Hemisphere, e.g., summertime convection over continents, which create summertime minima that reinforce the stratospheric signal (Liang et al., 2008; Ishijima et al., 2010). The observation that the strongest anti-correlations with stratospheric temperature are found in the month of or shortly after the surface minimum in the Northern Hemisphere but in months preceding the surface minimum in the Southern Hemisphere may result from the fact that the stratospheric signal begins to be felt in the troposphere near the peak of the oceanic thermal pulse in the Southern Hemisphere but several months before the thermal peak in the Northern Hemisphere. However, this is a speculative explanation.

Finally, our results have some implications for atmospheric N_2O inversions that attempt to resolve seasonality in fluxes. First, it seems likely that not all N_2O time series are equivalent in their ability to capture subtle seasonal and interannual variability, suggesting the importance of working closely with observationalists to determine limitations in data and appropriate measurement uncertainties. Our study also underscores the importance of accurately accounting for stratospheric and other remote transport influences, since these may be larger than biogeochemical source signals at many sites, especially those remote from local sources. This latter issue arguably is not fundamentally different for N_2O than for other atmospheric species, e.g., CO_2, for which transport model uncertainty led to a large range in the a posteriori seasonal fluxes of the Transcom-3 inversion (Gurney et al., 2004). However, the underlying mechanism for the CO_2 seasonal cycle is clearly biogeochemical (i.e., seasonal asynchrony in terrestrial photosynthesis and respiration), whereas for N_2O it likely is largely abiotic (i.e., the stratospheric influx).

5 Conclusions

Correlations between detrended tropospheric N_2O monthly mean data, sorted by month, and various interannually-varying proxies, including polar lower stratospheric temperature, polar vortex break-up date and coastal upwelling indices, are used to help identify the mechanisms that cause interannual variability in the N_2O seasonal cycle. In the months surrounding the N_2O seasonal minimum, the detrended N_2O data are significantly anti-correlated with winter polar lower stratospheric temperature at a number of Northern Hemisphere surface monitoring sites, with deeper minima and, in some cases, earlier onset of descent into the minima occurring in warm years, providing strong empirical evidence that these seasonal cycles bear a stratospheric influence. At Trinidad Head, California, detrended N_2O monthly means in summer are weakly correlated to the index for coastal upwelling, which ventilates N_2O-enriched deepwater to the atmosphere, but more strongly correlated after the stratospheric influence is accounted for using a multivariate regression against both stratospheric temperature and the coastal upwelling index. Monitoring sites in the extratropical Southern Hemisphere, where the stratospheric influence on surface N_2O has been more difficult to establish in previous studies, also show correlations between detrended N_2O monthly means and polar lower stratospheric temperature, although the anti-correlations generally are not centered on the month of the N_2O seasonal minimum as in the Northern Hemisphere, but rather are stronger in months preceding the minimum. Southern Ocean sites also are likely influenced by oceanic thermal and biological ventilation signals, although these influences are difficult to prove using the methodology of this study. N_2O seasonal cycles can vary strongly year to year, making a "mean" cycle difficult to define at some sites, especially those subject to competing influences from interannually-varying sources and the seasonal stratospheric influx. Among networks that share a common site, interannual variability in detrended N_2O monthly means is not necessarily well correlated, especially in the Northern Hemisphere. In part, this is a sampling issue, with weekly flask networks less able to detect subtle interannual signals and filter out noise due to atmospheric variability than more frequently sampled in situ networks. Due to the various abiotic influences on N_2O seasonal cycles, including thermal oceanic in and outgassing, the stratospheric influx, and tropospheric transport, complementary tracers like CFC-12 can help separate transport and stratospheric influences from soil and oceanic biogeochemical source signals, thus providing more insight into seasonality in N_2O sources than N_2O mixing ratio data alone.

Supplementary material related to this article is available online at:
http://www.atmos-chem-phys.net/11/3713/2011/acp-11-3713-2011-supplement.pdf.

Acknowledgements. CDN acknowledges support from NASA grant NNX08AB48G and thanks Paul Newman and Eric Nash for stratospheric data and Farahnaz Khosrawi, Qing Liang and Ralph Keeling for helpful comments. The authors are deeply grateful to the many people, from many organisations around the world, who have contributed to the production of the excellent N_2O datasets that have made this study possible. These include the people who diligently collect flask air samples, those who analyze the flask samples, and those staff who maintain the optimal operation and calibration of in situ instruments at baseline sites.

Edited by: J. Kaiser

References

Bouwman, A. F. and Taylor, J. A.: Testing high-resolution nitrous oxide emission estimates against observations using an atmospheric transport model, Global Biogeochem. Cy., 10, 307–318, 1996.

Bouwman, A. F., van der Hoek, K. W., and Olivier, J. G. J.: Uncertainties in the global source distribution of nitrous oxide, J. Geophys. Res., 100, 2785–2800, 1995.

Engel, A., Möbius, T., Haase, H.-P., Bönisch, H., Wetter, T., Schmidt, U., Levin, I., Reddmann, T., Oelhaf, H., Wetzel, G., Grunow, K., Huret, N., and Pirre, M.: Observation of mesospheric air inside the arctic stratospheric polar vortex in early 2003, Atmos. Chem. Phys., 6, 267–282, doi:10.5194/acp-6-267-2006, 2006.

Forster, P., Ramaswamy, V., Artaxo, P., Berntsen, T., Betts, R., Fahey, D. W., Haywood, J., Lean, J., Lowe, D. C., Myhre, G., Nganga, J., Prinn, R., Raga, G., Schulz, M., and Van Dorland, R.: Changes in Atmospheric Constituents and in Radiative Forcing, in: Climate Change 2007: The Physical Science Basis. Contribution of Working Group I to the Fourth Assessment Report of the Intergovernmental Panel on Climate Change, Cambridge University Press Cambridge, UK and New York, NY, USA, 2007.

Francey, R. J., Steele, L. P., Spencer, D. A., Langenfelds, R. L., Law, R. M., Krummel, P. B., Fraser, P. J., Etheridge, D. M., Derek, N., Coram, S. A., Cooper, L. N., Allison, C. E., Porter, L., and Baly, S.: The CSIRO (Australia) measurement of greenhouse gases in the global atmosphere, in: Baseline Atmospheric Program Australia 1999–2000, edited by: Tindale, N. W., Derek, N., and Fraser, P. J., Bureau of Meteorology and CSIRO Atmospheric Research, Melbourne, Australia, 42–53, 2003.

Glatthor, N., von Clarmann, T., Fischer, H., Funke, B., Grabowski, U., Hoepfner, M., Kellmann, S., Kiefer, M., Linden, A., Milz, M., Steck, T., Stiller, G. P., Mengistu Tsidu, G., and Wang, D.-Y.: Mixing processes duing the Antarctic vortex split in September–October 2002 as inferred from source gas and ozone distributions from ENVISAT-MIPAS, J. Atmos. Sci., 62(3), 787–800, 2005.

Gurney, K. R., Law, R. M., Denning, A. S., Rayner, P. J., Pak, B. C., Baker, D. F., Bousquet, P., Bruhwiler, L., Chen, Y.-H., Ciais, P., Fung, I. Y., Heimann, M., John, J., Maki, T., Maksyutov, S., Peylin, P., Prather, M., and Taguchi, S.: Transcom 3 inversion intercomparison: Model mean results for the estimation of seasonal carbon sources and sinks, Global Biogeochem. Cy., 18, GB1010, doi:10.1029/2003GB002111, 2004.

Hirsch, A. I., Michalak, A. M., Bruhwiler, L. M., Peters, W., Dlugokencky, E. J., and Tans, P. P.: Inverse modeling estimates of the global nitrous oxide surface flux from 1998–2001, Global Biogeochem. Cy., 20, GB1008, doi:10.1029/2004GB002443, 2006.

Holton, J. R., Haynes, P. H., McIntyre, M. E., Douglass, A. R., Rood, R. B., and Pfister, L.: Stratosphere-troposphere exchange, Rev. Geophys., 33(4), 403–439, 1995.

Huang, J., Golombek, A., Prinn, R., Weiss, R., Fraser, P., Simmonds, P., Dlugokencky, E. J., Hall, B., Elkins, J., Steele, P., Langenfelds, R., Krummel, P., Dutton, G., and Porter, L.: Estimation of regional emissions of nitrous oxide from 1997 to 2005 using multinetwork measurements, a chemical transport model, and an inverse method, J. Geophys. Res., 113, D17313, doi:10.1029/2007JD009381, 2008.

Ishijima, K., Patra, P. K., Takigawa, M., Machida, T., Matsueda, H., Sawa, Y., Steele, L. P., Krummel, P. B., Langenfelds, R. L., Aoki, S., and Nakazawa, T.: The stratospheric influence on the seasonal cycle of nitrous oxide in the troposphere as deduced from aircraft observations and model simulations, J. Geophys. Res., 115, D20308, doi:10.1029/2009JD013322, 2010.

Jiang, X., Ku, W. L., Shia, R.-L., Li, Q., Elkins, J. W., Prinn, R. G., and Yung, Y. L.: Seasonal cycle of N_2O: Analysis of data, Global Biogeochem. Cy., 21, GB1006, doi:10.1029/2006GB002691, 2007.

Jin, X. and Gruber, N.: Offsetting the radiative benefit of ocean iron fertilization by enhancing N_2O emissions, Geophys. Res. Lett., 30(24), 2249, 2003.

Jin, X., Najjar, R. G., Louanchi, F., and Doney, S. C.,: A modeling study of the seasonal oxygen budget of the global ocean, J. Geophys. Res., 112, C05017, doi:10.1029/2006JC003731, 2007.

Kalnay, E., Kanamitsu, M., Kistler, R., Collins, W., Deaven, D., Gandin, L., Iredell, M., Saha, S., White, G., Woollen, J., Zhu, Y., Leetmaa, A., Reynolds, R., Chelliah, M., Ebisuzaki, W., Higgins, W., Janowiak, J., Mo, K. C., Ropelewski, C., Wang, J., Jenne, R., and Joseph, D.: The NMC/NCAR 40-year reanalysis project, B. Am. Meteorol. Soc., 77, 437–471, 1996.

Khosrawi, F., Mueller, R. Proffitt, M. H., Urban, J., Murtagh, D., Ruhnke, R., Grooß, J.-U., and Nakajima, H.: Seasonal cycle of averages of nitrous oxide and ozone in the Northern and Southern Hemisphere polar, midlatitude, and tropical regions derived from ILAS/ILAS-II and Odin/SMR observations, J. Geophys. Res., 113, D18305, doi:10.1029/2007JD009556, 2008.

Kroeze, C., Mosier, A., and Bouwman, L.: Closing the global N_2O budget: A retrospective analysis 1500–1994, Global Biogeochem. Cy., 13, 1–8, 1999.

Lambert, A., Read, W. G., Livesey, N. J., Santee, M. L., Manney, G. L., Froidevaux, L., Wu, D. L., Schwartz, M. J., Pumphrey, H. C., Jimenez, C., Nedoluha, G. E., Cofield, R. E., Cuddy, D. T., Daffer, W. H., Drouin, B. J., Fuller, R. A., Jarnot, R. F., Knosp, B. W., Pickett, H. M., Perun, V. S., Snyder, W. V., Stek, P. C., Thurstans, R. P., Wagner, P. A., Waters, J. W., Jucks, K. W., Toon, G. C., Stachnik, R. A., Bernath, P. F., Boone, C. D., Walker, K. A., Urban, J., Murtagh, D., Elkins, J. W., and Atlas, E.: Validation of the Aura Microwave Limb Sounder middle atmosphere water vapor and nitrous oxide measurements, J. Geophys. Res., 112, D24S36, doi:10.1029/2007JD008724, 2007.

Liang, Q., Stolarski, R. S., Douglass, A. R., Newman, P. A., and Nielsen, J. E.: Evaluation of emissions and transport of CFCs using surface observations and their seasonal cycles and the GEOS CCM simulation with emissions-based forcing, J. Geophys. Res., 113, D14302, doi:10.1029/2007JD009617, 2008.

Liang, Q., Douglass, A. R., Duncan, B. N., Stolarski, R. S., and Witte, J. C.: The governing processes and timescales of stratosphere-to-troposphere transport and its contribution to ozone in the Arctic troposphere, Atmos. Chem. Phys., 9, 3011–3025, doi:10.5194/acp-9-3011-2009, 2009.

Lovenduski, N. S., Gruber, N., Doney, S. C., and Lima, I. D.: Enhanced CO_2 outgassing in the Southern Ocean from a positive phase of the Southern Annular Mode, Global Biogeochem. Cy., 21, GB2026, doi:10.1029/2006GB002900, 2007.

Lueker, T. J., Walker, S. J., Vollmer, M. K., Keeling, R. F., Nevison, C. D., and Weiss, R. F.: Coastal upwelling air-sea fluxes revealed in atmospheric observations of O_2/N_2, CO_2 and N_2O, Geophys. Res. Lett., 30, 1292, 2003.

MacFarling Meure, C., Etheridge, D. M., Trudinger, C. M., Steele, L. P., Langenfelds, R. L., van Ommen, T., Smith, A., and Elkins, J. W.: Law Dome CO_2, CH_4, and N_2O ice core records extended to 2000 years BP, Geophys. Res. Lett., 33, L14810, doi:10.1029/2006GL026152, 2006.

Mahowald, N. M., Rasch, P. J., Eaton, B. E., Whittlestone, S., and Prinn, R. G.: Transport of radon-222 to the remote troposphere using the Model of Atmospheric Transport and Chemistry and assimilated winds from ECMWF and the National Center for Environmental Prediction/NCAR, J. Geophys. Res., 102, 28139–28151, 1997.

Mosier, A. R., Duxbury, J. M., Freney, J. R., Heinemeyer, O., and Minami, K.: Assessing and mitigating N_2O emissions from agricultural soils, Climatic Change, 40, 7–38, 2000.

Naqvi, S. W. A., Jayakumar, D. A., Narvekar, P. V., Naik, H., Sarma, V. V. S. S., D'Sousa, W., Joseph, S., and George, M. D.: Increased marine production of N_2O due to intensifying anoxia on the Indian continental shelf, Nature, 408, 346–349, 2000.

Nash, E. R., Newman, P. A., Rosenfield, J. E., and Schoeberl, M. R.: An objective determination of the polar vortex using Ertel's potential vorticity, J. Geophys. Res., 101, 9471–9478, 1996.

Nevison, C. D., Weiss, R. F. and Erickson III, D. J.: Global Oceanic Nitrous Oxide Emissions, J. Geophys. Res., 100, 15809–15820, 1995.

Nevison, C. D., Kinnison, D. E., and Weiss, R. F.: Stratospheric Influence on the tropospheric seasonal cycles of nitrous oxide and chlorofluorocarbons, Geophys. Res. Lett., 31(20), L20103, doi:10.1029/2004GL020398, 2004.

Nevison, C. D., Keeling, R. F., Weiss, R. F., Popp, B. N., Jin, X., Fraser, P. J., Porter, L. W., and Hess, P. G.: Southern Ocean ventilation inferred from seasonal cycles of atmospheric N_2O and O_2/N_2 at Cape Grim, Tasmania, Tellus B, 57, 218–229, 2005.

Nevison, C. D., Mahowald, N. M., Weiss, R. F., and Prinn, R. G.: Interannual and seasonal variability in atmospheric N_2O, Global Biogeochem. Cy., 21, GB3017, doi:10.1029/2006GB002755, 2007.

Nevison, C. D., Keeling, R. F., Kahru, M., Manizza, M., Mitchell, B. G., Cassar, N.: Estimating net community production in the Southern Ocean based on Atmospheric Potential Oxygen and satellite ocean color data, submitted to Global Biogeochem. Cy., 2011.

Olivier, J. G. J., Van Aardenne, J. A., Dentener, F., Ganzeveld, L., and Peters, W.: Recent trends in global greenhouse gas emissions: regional trends and spatial distribution of key sources, in: Non-CO_2 Greenhouse Gases (NCGG-4), edited by: van Amstel, A., Millpress, Rotterdam, 325–330, 2005.

Orsi, A. H., Whitworth III, T., and Nowlin Jr., W. D.: On the meridional extent and fronts of the Antarctic Circumpolar Current, Deep-Sea Res. Pt. I, 42(5), 651–673, 1995.

Prinn, R. G., Weiss, R. F., Fraser, P. J., Simmonds, P. G., Cunnold, D. M., Alyea, F. N., O'Doherty, S., Salameh, P., Miller, B. R., Huang, J., Wang, R. H. J., Hartley, D. E., Harth, C., Steele, L. P., Sturrock, G., Midgley, P. M., and McCulloch, A.: A history of chemically and radiatively important gases in air deduced from ALE/GAGE/AGAGE, J. Geophy. Res., 105(D14), 17751–17792, 2000.

Ravishankara, A. R., Daniel, J. S., and Portmann, R. W.: Nitrous Oxide (N_2O): The dominant ozone depleting substance emitted in the 21st century, Science, 326, 123–125, doi:10.1126/science.1176985, 2009.

Sokal, R. R. and Rohlf, F. J.: Biometry, W. H. Freeman, New York, 859 pp., 1981.

Stohl, A.: A 1-year Lagrangian "climatology" of airstreams in the Nor thern Hemisphere tropo- sphere and lowermost stratosphere, J. Geophys. Res., 106(D7), 7263–7279, 2001.

Thompson, T. M., Elkins, J. W., Hall, B., Dutton, G. S., Swanson, T. H., Butler, J. H., Cummings, S. O., and Fisher, D. A.: Halocarbons and other Atmospheric Trace Species, in: Climate Diagnostics Laboratory Summary Report #27, 2002–2003, edited by: Schnell, R. C., Buggle, A.-M., and Rossson, R. M., US Department of Commerce, National Oceanic and Atmospheric Administration, Boulder, Colorado, 2004.

Volk, C. M., Elkins, J. W., Fahey, D., Dutton, G., Gilligan, J., Lowenstein, M., Podolske, J., Chan, K., and Gunson, M.: Evaluation of source gas lifetimes from stratospheric observations, J. Geophys. Res., 102(D21), 25543–25564, 1997.

Waugh, D. W., Randel, W. J., Pawson, S., Newman, P. A., and Nash, E. R.: Persistence of the lower stratospheric polar vortices, J. Geophys. Res., 104(D22), 27191–27201, 1999.

Weiss, R. F.: The temporal and spatial distribution of tropospheric nitrous oxide, J. Geophys. Res., 86, 7185–7195, 1981.

Wofsy, S. C., the HIPPO Science Team and Cooperating Modellers and Satellite Teams: HIAPER Pole-to-Pole Observations (HIPPO): Fine grained, global scale measurements for determining rates for transport, surface emissions, and removal of climatically important atmospheric gases and aerosols, Philos. T. Roy. Soc. A, 369(1943), doi:10.1098/rsta.2010.0313, 2073–2086, 2011.